Elastic scattering and direct reactions of the 1n halo ^{11}Be nucleus on ^{64}Zn near the barrier

2012 J. Phys.: Conf. Ser. 381 012050

(http://iopscience.iop.org/1742-6596/381/1/012050)

Journal of Physics: Conference Series **381** (2012) 012050 doi:10.1088/1742-6596/381/1/012050

Elastic scattering and direct reactions of the 1n halo ^{11}Be nucleus on ^{64}Zn near the barrier

V. Scuderi[1,2], A. Di Pietro[2], L. Acosta[3], F. Amorini[1,2], M.J.G. Borge[4], P. Figuera[2], M. Fisichella[1,2], L. M. Fraile[5†], J. Gomez-Camacho[6], H. Jeppesen[5§], M. Lattuada[1,2], I. Martel[3], M. Milin[7], A. Musumarra[2,8], M. Papa[2], M.G. Pellegriti[1,2], F. Perez-Bernal[3], R. Raabe[9],G. Randisi[1,2‡], F. Rizzo[1,2], D. Santonocito[2], G. Scalia[1,2], O. Tengblad[4], D. Torresi[1,2], A.M. Vidal[4], M. Zadro[10]

1Dipartimento di Fisica ed Astronomia Università di Catania, Catania, Italy

2INFN-Laboratori Nazionali del Sud and Sezione di Catania, Italy

3Departamento de Fisica Aplicada Universidad de Huelva, Huelva, Spain

4Instituto de Estructura de la Materia CSIC, Madrid, Spain

5CERN, Geneva, Switzerland

6Departamento de Fisica Atomica Molecular Nuclear Universidad de Sevilla, Sevilla, Spain

7Department of Physics Faculty of Science University of Zagreb, Zagreb, Croatia

8Dipartimento di Metodologie Fisiche e Chimiche per l'Ingegneria Università di Catania,Catania, Italy

9Instituut voor Kern-en Stralingsfysica University of Leuven, Leuven, Belgium

10Division of Experimental Physics Ruder Boskovic Institute, Zagreb, Croatia

scuderiv@lns.infn.it

Abstract. Elastic scattering and direct reactions have been studied for the collisions induced by the three Beryllium isotopes ^{9,10,11}Be, on a medium mass ^{64}Zn target at energies near the Coulomb barrier. The elastic-scattering angular distribution of the ^{11}Be halo nucleus shows a deviation from the classical Fresnel type diffraction behavior in the Coulomb-nuclear interference peak angular region. The deduced total reaction cross-sections for the ^{11}Be collision is more than a factor of two than the ones measured in the collisions induced by $^{9;10}$Be. Moreover, for ^{11}Be a large contribution to the total reaction cross-section due to transfer and break-up processes has been observed.

1. Introduction

Elastic scattering and reaction mechanisms around the barrier in collisions induced by halo nuclei have been the object of many publications in the last years (see e.g. [1-3] and references therein) in the attempt to investigate both the influence of the projectile halo structure and the effect of the break-up coupling on the reaction dynamics. Hundred years after Rutherford's α scattering experiment [4], elastic scattering turned out to be a very suitable tool to study peculiar nuclear structures as for instance the nuclear halo. Since elastic scattering is a peripheral process it can give information on the tail of the wave-function and hence one can learn about surface properties such as sizes of nuclei and surface diffuseness and how they can affect the shape of the projectile-target potential.

As it is well known, the peculiar structure of halo nuclei, which have an extended matter distribution and a very low binding energy, are expected to strongly affect the reaction mechanisms [1-3], especially at energies around the Coulomb barrier where couplings between the entrance channel and the continuum [5-9], as well as to the various reaction channels [2,3,10,11] are expected to be very important. Direct processes, such as break-up or transfer, may be favored owing to the low break-up threshold, the extended tail of halo nuclei and the large Q-values for selected transfer channels.

From an experimental point of view, high quality data are necessary, however, due to the low intensities of the radioactive beams, these are not always available. Since ^{6}He beams are available in different facilities with intensities up to 10^{7} pps, in a wide range of energies, almost all elastic-scattering studies around the barrier with halo nuclei have been performed so far with the 2n halo nucleus ^{6}He on several targets [12, 13]. A common feature, observed in the ^{6}He induced elastic scattering, is a reduction of the cross-section in most of the measured angular range [12, 13]. As a consequence of the elastic cross-section suppression, the total reaction (TR) cross-section is found to be much larger, a factor of 2 in some cases, than the one observed in reactions induced by non-halo nuclei [11, 12, 14].

To our knowledge, only three papers exist concerning elastic scattering around the barrier with n-halo nuclei different than ^{6}He [15, 16, 17]. In [15] ^{11}Be+^{120}Sn quasi-elastic scattering was measured but in a very limited angular range. In [16] quasi elastic scattering of ^{11}Be on ^{209}Bi has been measured. Due to the lack of post accelerated ^{11}Be beams, the authors were forced to use a fragmentation beam of ^{11}Be degraded to barrier energies. The TR cross-sections extracted from the analysis of the quasi-elastic angular distributions were compared with the ones for the system ^{9}Be+^{209}Bi finding similar values at energies exceeding 10% the barrier [16], result which appears to be different to what observed in the literature in ^{6}He induced collisions.

In the last years, thanks to the availability of a pure and post-accelerated ^{11}Be beam at Rex-Isolde facility of CERN, we have measured the elastic scattering angular distributions for the collisions induced by the three different Be isotopes, ^{9,10,11}Be, on a medium mass ^{64}Zn target in a wide angular range and with small angular step at $E_{c.m.}$= 24.5 MeV, close to the Coulomb barrier [17]. By comparing the elastic-scattering angular distributions for these three systems, the separate effect of the halo structure can be investigated. Moreover, in the case of the ^{11}Be the transfer/break-up cross-section has been measured, as well.

2. Experimental apparatus

The experiment with the stable ^{9}Be beam was performed at Laboratori Nazionali del Sud (LNS) in Catania. The ^{9}Be beam was delivered by the SMP 14MV Tandem of LNS and was impinging on a 550 μm/cm^{2} ^{64}Zn. The light charged particles, emitted in the reaction, have been detected using five ΔE (~10 μm thick) - E (~ 150 μm thick) Si detector telescopes each consisting of a surface barrier detector. The five telescopes were placed on a rotating support allowing the measurement of the elastic scattering angular distribution up to 110°.

The detection system for the experiments performed with the radioactive ^{10,11}Be beams at REX-ISOLDE, shown in fig. 1, consists of 6 ΔE (~ 50 μm thick) - E (~ 1500 μm thick) Si detector telescopes, each one with a surface of 50x50mm^{2}, surrounding a thin ^{64}Zn target (550 μg/cm2 and

1000 μg/cm^2 for the ^{10,11}Be beams, respectively). The targets were tilted at 45° to allow the measurement in the angular region around 90°. The ΔE stage consists of a Double sided Silicon Strip Detector (DsSSD) segmented in 16 strips both on the front side and on the rear side, allowing a 256 pixels for each detector. The E stage consists of a Silicon Single Pad detector. The total angular range covered by the set-up was between 10°<θ<150°. The average beam intensity was 10^6 pps and 10^4 pps for ^{10}Be and ^{11}Be, respectively.

Since, in order to have a large polar angle and solidangle coverage, the detectors were placed very close to the target small variations of the beam spot position onto the target resulted in a large variation of the detector angles. Therefore, to reconstruct the correct detector angles we have looked at the small angle Rutherford scattering in the two front detectors placed symmetrically with respect the beam axis. In order to check the adopted procedure, we measured the elastic scattering angular distributions for the reactions ^{12}C, ^{10}Be + ^{197}Au at E_{lab}= 28 and 29.4 MeV, respectively, and we obtained the expected Rutherford behavior of the cross-sections.

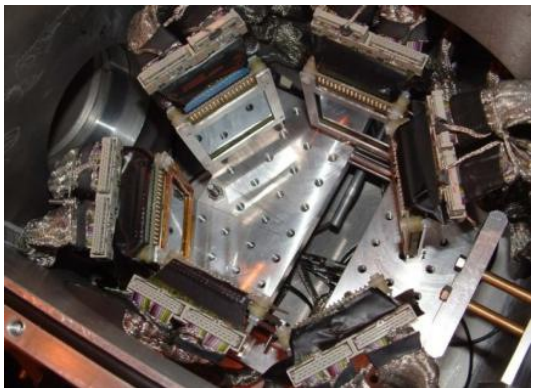

Figure 1. Picture of the detector set-up inside the scattering chamber.

3. Results

Fig. 2 shows the angular distributions for the scattering of ^{9,10,11}Be+^{64}Zn in linear scale. We must say that, as in [16], also in the present case the ^{11}Be+^{64}Zn scattering cross-section is the quasi elastic cross-section, since the inelastic contribution of the 1st excited state of ^{11}Be at E_x=320 keV is included. However, the inelastic scattering contribution has been evaluated by calculating the Coulomb excitation cross-section performing Optical Model (OM) calculations with the potential parameters extracted from the fit of the ^{11}Be scattering data and the coupling strength determined from the experimental transition probability B(E1)=0.115e^{2}fm^2 [18]. According to these calculations, as it can be seen in the inset of fig. 2, the inelastic contribution to the scattering cross-section is quite small at all measured angles and therefore negligible. For this reason we refer to the angular distribution for ^{11}Be+^{64}Zn as elastic scattering angular distribution.

As one can see from fig. 2, in spite of the very different binding energies of ^{9}Be and ^{10}Be isotopes, their elastic-scattering angular distributions appear to be very similar and they both show the standard Fresnel type diffraction behaviour. On the contrary, ^{11}Be scattering data shows a very different pattern and the main feature that one can observe is a strong reduction of the elastic cross-section at forward angles. In [5] the deviation of the elastic scattering angular distribution from the standard Fresnel type diffraction pattern has been investigated for the ^{6}He projectile on several target charges and beam energies. This deviation has been related to the strong coupling with a large Coulomb dipole excitation due to the presence of the low-lying electric dipole strength. However, the authors concluded that at energies close to the Coulomb barrier the effect of the coupling to the Coulomb dipole break-up should be evident only in scattering with targets having high charge (Z_T ~ 80), i.e. in the presence of

large Coulomb field, and that measurements with lighter targets ($Z_T \sim 28$) are not sensitive to this coupling. Indeed, in the ^{6}He induced collisions, a clear reduction of elastic cross-section at forward angles has been observed although not as large as in the present case and only for heavy targets [13]. The elastic scattering angular distribution of ^{6}He on a medium mass target ^{64}Zn does not show such feature [12]. Therefore, the observation of a strong reduction of elastic cross-section at small angles in the scattering of ^{11}Be, which has a strong low-lying continuum dipole strength as ^{6}He and ^{9}Be, with a light charge target has to be attributed to other mechanisms besides coupling to Coulomb break-up, that could be associated with the halo structure. Recently, in [19] it has been shown, by means of Continuum Discretized Coupled Channel (CDCC) calculations, that the suppression of the Coulomb nuclear interference peak [20] in the measured ^{11}Be+^{64}Zn angular distribution is mainly caused by the nuclear coupling to the continuum. The authors concluded that, although the Coulomb break-up coupling does make an important contribution, it is not of primary importance in reproducing the absence of the Coulomb-nuclear interference peak as in the case of the ^{6}He on heavy targets [13].

We have analysed the ^{9,10,11}Be+^{64}Zn elastic-scattering data within the OM framework using the code PTOLEMY [21]. For ^{9,10}Be a Woods-Saxon (W-S) form to describe both the real and the imaginary part of the potential was used. In the case of ^{11}Be, the volume potential, responsible for the inelastic core-target interaction, was obtained from the fit of the elastic-scattering of the core ^{10}Be on ^{64}Zn. In order to take into account the coupling to the continuum, in addition to the imaginary part of the volume potential, a phenomenological dynamic polarization potential consisting of a surface term having the shape of a Woods-Saxon derivative was considered. In order to avoid a fit with too many free parameters, only the depth and diffuseness of the surface imaginary term were varied in the fits. The effect of the surface imaginary term is to reduce the scattering cross-section at all the measured angles and in particular in order to reproduce the observed suppression in the region of the Coulomb-nuclear interference peak a very large surface diffuseness parameter, of the order of 3.5 fm, was needed. Such value is in qualitative agreement with the calculations of [22]. The large diffuseness confirms the presence of long range absorption mechanisms. More details on the OM analysis and the potential parameters are reported in [17].

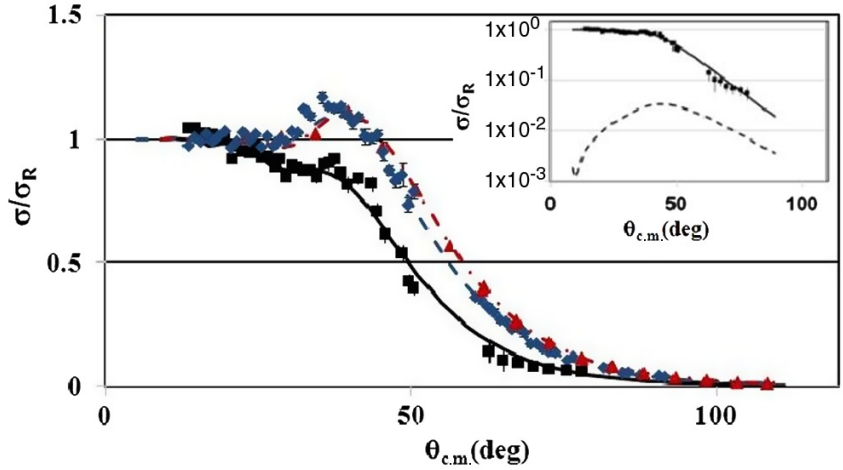

Figure 2. Elastic-scattering angular distributions on ^{64}Zn: ^{9}Be(triangles), ^{10}Be (diamonds) and ^{11}Be (squares). The lines represent the OM calculations for ^{9}Be(dot dashed), ^{10}Be (dashed) and ^{11}Be (full line). The inset shows the measured angular distribution (symbols) and OM fit (full line) for the ^{11}Be+^{64}Zn system together with the result of the calculation for the inelastic excitation of ($1/2^-$, E_x = 0.32 MeV, dashed line).

The TR cross-sections deduced from the OM analysis are $\sigma_{TR} \sim 1$ b for ^{9}Be, $\sigma_{TR} \sim 1.2$ b for ^{10}Be and $\sigma_{TR} \sim 2.7$ b for ^{11}Be. The observed enhancement of the TR cross section for the halo ^{11}Be nucleus with

respect to the other two isotopes is in qualitative agreement to what has been observed by different authors for ^{6}He on several targets.

Since the TR cross-section for the ^{11}Be case is much larger, more than a factor of two, than the one for the ^{9,10}Be, it is important to understand if such enhancement could be due to direct processes as for the ^{6}He induced reactions [12, 14, 23]. Indeed, looking at the ΔE-E spectra for the reactions induced by ^{10}Be and ^{11}Be, shown in fig. 3 (a), one can notice, in the ^{11}Be case, events close to the elastic and consistent with the detection of ^{10}Be coming from direct processes, like for instance transfer and break-up, which are not present in the corresponding spectra with the ^{10}Be beam. The angular distribution for such events is shown in fig. 3 (b). The corresponding integrated cross-section is about 1b. This cross-section corresponds to about 40% of the TR cross-section measured for ^{11}Be. This result confirm that in the ^{11}Be case direct processes are giving a large contribution to the TR cross section as observed in the ^{6}He experiments (e.g. [12, 23]).

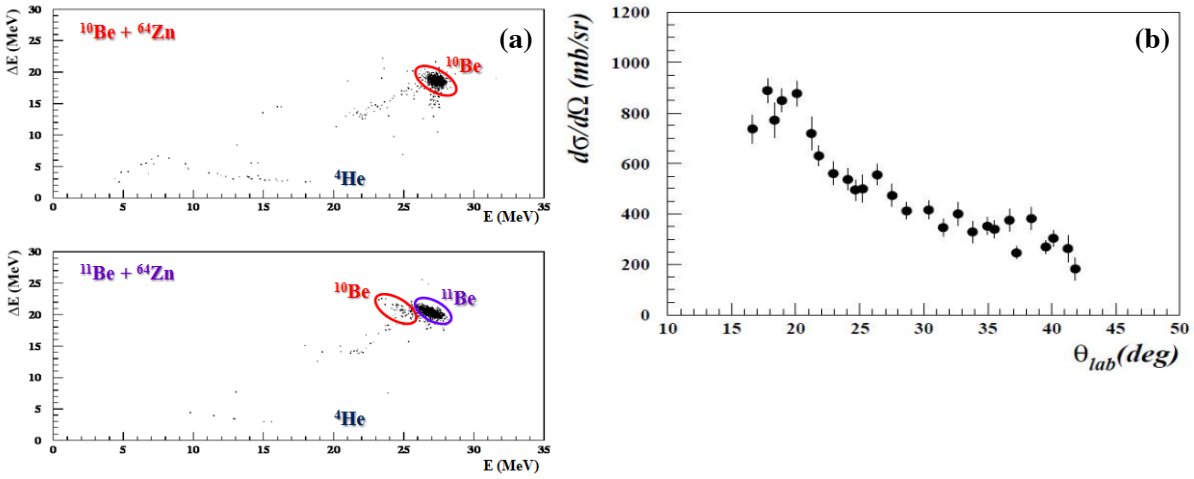

Figure 3. (a) Δ*E*-*E* spectra for the reactions ^{10}Be+^{64}Zn (top) and ^{11}Be+^{64}Zn (bottom), at θ=35°. **(b)** Angular distribution of transfer/break-up events in ^{11}Be+^{64}Zn obtained by selecting ^{10}Be events in the ΔE-E spectrum.

4. Conclusion

In conclusion, we have studied the collisions ^{9,10,11}Be + ^{64}Zn at energy close to the Coulomb barrier using for the first time high quality post-accelerated beams. The scattering of the ^{11}Be halo nucleus shows extremely different features with respect the ^{9}Be and ^{10}Be. The ^{11}Be elastic cross-section is strongly suppressed in particular in the Coulomb nuclear interference peak angular range indicating that absorption occurs at much smaller scattering angles than for the other two Be isotopes.

All the scattering data were interpreted within the OM. In order to take into account the ^{11}Be diffuse halo structure and to reproduce the scattering data a surface imaginary potential with a very large diffuseness parameter was needed. Along with the OM parameters the TR cross-section were also extracted and a much larger TR cross-section was found in the ^{11}Be halo nucleus case than for the ^{9,10}Be induced reactions. Moreover, from the analysis of ^{10}Be events, detected in the collision induced by the ^{11}Be halo nucleus, about 40% of the TR cross-section has been attributed to transfer and/or break-up processes.

These results shows a strong effect on nuclear reaction mechanisms around the barrier due to the ^{11}Be halo structure and represents an independent confirmation that similar effects observed for the ^{6}He are also due to its halo nature.

References

[1] L. F. Canto et al., Phys. Rep. 424, 1, (2006).
[2] N. Keeley et al., Prog. Part. Nucl. Phys. 59, 579, (2007).
[3] N. Keeley et al., Prog. Part. Nucl. Phys. 63, 396, (2009).
[4] E. Rutherford, Philos. Mag. 21, 669 (1911).
[5] Y. Kucuk et al., Phys. Rev. C 79, 067601 (2009).
[6] A. Moro et al., Phys. Rev. C 75, 064607 (2007).
[7] T. Matsumoto et al., Phys. Rev. C 73, 051602R (2006).
[8] M. Rodriguez-Gallardo et al., Phys. Rev. C 77, 064609 (2008).
[9] K. Rusek et al., Phys. Rev. C 72, 037603 (2005).
[10] N. Keeley and N. Alamanos, Phys. Rev. C 77, 054602 (2008).
[11] A. Chatterjee et al., Phys. Rev. Lett. 101, 032701 (2008).
[12] A. Di Pietro et al., Phys. Rev. C 69, 044613 (2004).
[13] A. M. Sanchez-Benitez et al., Nucl. Phys. A 803, 30 (2008).
[14] E. Aguilera et al., Phys. Rev. C 63, 061603(R) (2001).
[15] L. Acosta et al., Eur. Phys. Jour. A42, 461, (2009).
[16] M. Mazzocco et al, Eur. Phys. Jour. S.T. 150, 37, (2007).
[17] A. Di Pietro et al., Phys. Rev. Lett. 105, 022701, (2010).
[18] F. Ajzenberg-Selove, Nucl. Phys. A506, 1 (1990).
[19] N.Keeley et al., Phys.Rev. C 82, 034606 (2010)
[20] S. Fricke et al., Nucl. Phys. A500, 399 (1989).
[21] M. Rhoades-Brown et al., Phys. Rev. C 21, 2417 (1980).
[22] A. Bonaccorso and F. Carstoiu, Nucl. Phys. A 706, 322 (2002).
[23] P. D. Young et al., Phys. Rev. C 71, 051601R (2005).